THE JOURNAL OF PHYSICAL CHEMISTRY B

ARTICLE

pubs.acs.org/JPCB

Dielectric Relaxation Spectroscopy for Evaluation of the Influence of Solvent Dynamics on Ion Transport in Succinonitrile−Salt Plastic Crystalline Electrolytes

Supti Das and Aninda J. Bhattacharyya*

Solid State and Structural Chemistry Unit, Indian Institute of Science, Bangalore 560012, India

Supporting Information

ABSTRACT: Influence of succinonitrile (SN) dynamics on ion transport in SN−lithium perchlorate ($LiClO_4$) electrolytes is discussed here via dielectric relaxation spectroscopy. Dielectric relaxation spectroscopy (~2×10^{-3} Hz to 3 MHz) of SN and SN−$LiClO_4$ was studied as a function of salt content (up to 7 mol % or 1 M) and temperature (−20 to +60 °C). Analyses of real and imaginary parts of permittivity convincingly reveal the influence of trans−gauche isomerism and solvent−salt association (solvation) effects on ion transport. The relaxation processes are highly dependent on the salt concentration and temperature. While pristine SN display only intrinsic dynamics (i.e., trans−gauche isomerism) which enhances with an increase in temperature, SN−$LiClO_4$ electrolytes especially at high salt concentrations (~0.04−1 M) show salt-induced relaxation processes. In the concentrated electrolytes, the intrinsic dynamics was observed to be a function of salt content, becoming faster with an increase in salt concentration. Deconvolution of the imaginary part of the permittivity spectra using Havriliak−Negami (HN) function show a relaxation process corresponding to the above phenomena. The permittivity data analyzed using HN and Kohlrausch−Williams−Watta (KWW) functions show non-Debye relaxation processes and enhancement in the trans phase (enhanced solvent dynamics) as a function of salt concentration and temperature.

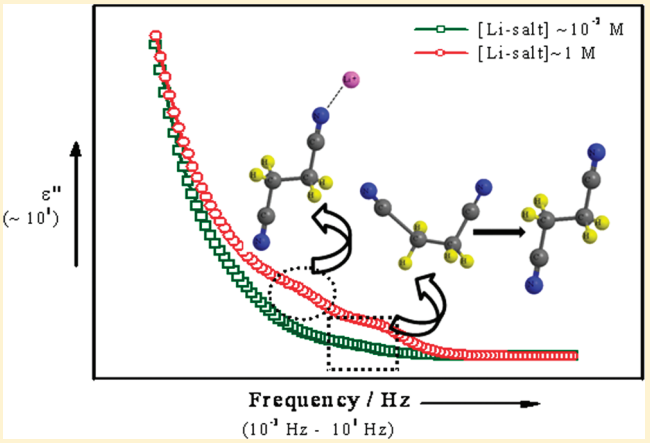

1. INTRODUCTION

Soft mater ion conductors[1−7] provide multiple opportunities for the development of solid-state electrochemical devices such as rechargeable lithium batteries.[8,9] High ionic conductivity of the electrolyte is a necessary criteria for consideration in practical devices, and this criterion is well-satisfied in the case of gel[7,10,11] and polymer electrolytes,[4,10] which show conductivity ~ 10^{-5}−10^{-3} Ω^{-1} cm^{-1}. In recent times emphasis has shifted from molecular liquid solvent and polymer-based electrolytes to low melting point solids such as ionic liquids[6] and plastic crystalline electrolytes.[12−16] Ionic liquids and plastic crystalline electrolytes possess ambient temperature ionic conductivity similar to molecular liquid electrolytes and exhibit a wide electrochemical voltage window and higher safety. Plasticity is an important physical phenomenon and has been observed in a wide range of solid materials, from inorganic (including metals)[17−19] to organic molecules (including low melting point solids).[20] The origin of plasticity is attributed to the presence of orientational disorder at lattice points which originates above a transition temperature characteristic of the material. While in metals and inorganic materials transformation to the plastic phase occurs at far higher temperatures than ambient, organic compounds exhibit plasticity at ambient or near-ambient temperature regimes (≤100 °C). This is highly beneficial for applications in electrochemical devices as they operate at ambient temperatures. An argument often invoked is that the concentrations of point defects and dislocations are considerably enhanced as a result of initiation of orientational disorder. This leads to enhancement in ionic conductivity by several orders of magnitude in the plastic phase compared to the normal crystalline phase. However, this is a strong proposition only in the case of solids which are highly ordered (crystalline) below the transition temperature. As the organic plastic crystalline materials of interest (e.g., pyrolidinium, imidazolium, and succinonitrile) are predominantly amorphous, a more realistic approach to comprehension of ion transport would be via concepts typically applicable to liquid. Strong evidence in support of this approach is that similar to polymer electrolytes, in the case of low melting point solids, in particular plastic crystalline materials, macroscopic material properties are governed by solvent parameters such as solvent dynamics and solvation. Hence, understanding ion transport of plastic crystalline based on liquid concepts should necessarily involve the study

Received: September 16, 2010
Revised: December 15, 2010
Published: February 22, 2011

of various relaxation processes of the solvent and ionic species present in the electrolyte.

We now turn our attention to a specific plastic crystalline system which is of both fundamental and applied interests. Succinonitrile (SN, N≡C—CH_2—CH_2—C≡N)[12,14−16,21] is a highly polar waxlike solid organic molecular plastic material (dielectric constant, ε = 55). In contrast to the undoped Py/Im based plastic electrolytes, pristine SN is almost an insulator in its plastic phase temperature regime (∼−35 to +60 °C). The plastic phase is marked by two molecular conformations, viz., majority gauche (∼70−80%) and minority trans (20−30%) approximately[22] and has been demonstrated to be an excellent solvent for dissolution of a large variety of salts. The trans−gauche isomerism results from the ensuing rotation about the central C−C bond. Recently, the crystallographic structure in the plastic phase has been demonstrated to be a function of the salt concentration.[21] At temperature below normal to plastic crystalline temperature, T_{cp}, succinonitrile freezes in gauche conformation in the monoclinic crystallographic structure. SN-based electrolytes conduct only in the plastic phase regime, and this has been attributed to the solvent dynamics, i.e., trans−gauche isomerism.

In this work, we employ dielectric relaxation spectroscopy to study the various relaxation processes of the solvent and ions responsible for ion transport in succinonitrile-based solid electrolytes. Dielectric relaxation spectroscopy[23−25] has been demonstrated to be a powerful method in the studies of solvent dynamics in pure liquid and polymer electrolytes. Here we elucidate the influence of salt and temperature on succinonitrile trans−gauche isomerism (solvent dynamics) via study of the frequency dependence of dielectric function. The dielectric relaxation studies were performed on succinonitrile−lithium perchlorate (SN−$LiClO_4$), a representative SN-based electrolyte. The permittivity data are further analyzed using Havriliak−Negami (HN) and Kohlrausch−Williams−Watta (KWW) functions for identification of various processes and also for detailed insight on the ion transport mechanism.

2. EXPERIMENTAL MATERIALS AND METHODS

Prior to the electrolyte preparation succinonitrile (Aldrich) was sublimated twice to remove impurities, and lithium perchlorate ($LiClO_4$, lithium battery grade, Chemetall GmBH) was preheated at 110 °C under vacuum to rule out effects arising out of physisorped water. The plastic crystalline electrolyte was prepared by adding a requisite amount of $LiClO_4$ (x = 0.005−1 M or 0−7 mol %) in molten SN and stirred at 60 °C (under dry N_2 atmosphere) until a homogeneous mixture was obtained. Homogeneous transparent samples were obtained for all concentrations of $LiClO_4$. The solidified melt was stored in glass vials under vacuum at 25 °C until further use.

Impedance spectra (Novocontrol Alpha-A) recorded over the frequency range of 2 × 10^{-3} Hz to 3 MHz (signal amplitude, 0.05 V) were utilized to obtain dielectric permittivity (ε^*). The real (ε') and imaginary (ε'') components are related to complex permittivity and impedance via the following relations.

$$\varepsilon^* = \varepsilon' - i\varepsilon'' \tag{1}$$

where

$$\varepsilon' = \frac{-Z'' C_R}{2\pi f \varepsilon_0((Z')^2 + (Z'')^2)} \tag{1a}$$

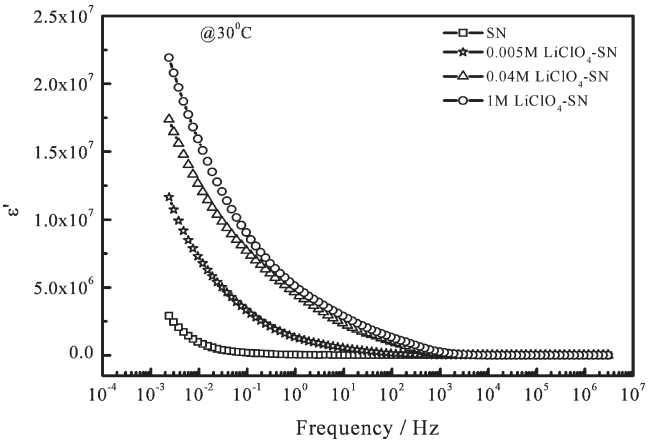

Figure 1. Variation of real part of dielectric permittivity (ε') as a function of frequency for 0−1 M $LiClO_4$−SN at 30 °C.

$$\varepsilon'' = \frac{-Z' C_R}{2\pi f \varepsilon_0((Z')^2 + (Z'')^2)} \tag{1b}$$

C_R is the cell constant, ε_0 is vacuum permittivity, f is frequency, and Z' and Z'' are the real and imaginary parts of impedance, respectively.

For dielectric measurement, samples in the molten form were poured into a home-built conductivity glass cell. The glass cell was then housed inside an outer glass jacket. Following this the jacket was evacuated (pressure = 1 mbar). This implied that the conductivity glass cell was effectively housed under vacuum. The cell and jacket combination was subsequently immersed in a thermostat (FP50MC Julabo) containing a water−ethylene glycol (1:1 (v/v)) mixture. Impedance spectra in the requisite frequency range (described above) were recorded as a function of temperature (−20 to +60 °C). All cells for dielectric relaxation measurement were assembled inside a glovebox (MBraun MB 20G LMF; water, ≤0.1 ppm) with argon atmosphere.

3. RESULTS AND DISCUSSION

Figure 1 shows the variation of the real part of the dielectric permittivity, ε' (dielectric constant), as a function of frequency for pristine SN and x M $LiClO_4$−SN (x = 0.005−1) electrolytes at 30 °C. Figure 1 shows an increase in value of dielectric permittivity with an increase in the salt concentration. In general, the increase in dielectric constant at low frequencies is due to space charge polarization. In the present study, free charge carriers increase with the increase in salt concentration. This increase leads to an increase in the space charge effect and hence the dielectric constant.[26,27] This observation also agrees well with extensive ionic conductivity and Fourier transform infrared studies reported earlier.[21] The variation of dielectric permittivity as a function of frequency at different temperature for pristine SN and x M $LiClO_4$−SN electrolytes is shown in Figure 2. The real part of the dielectric permittivity reveals only one relaxation process for pure SN at 60 °C. This relaxation process is attributed to the intrinsic trans−gauche isomerism of the SN molecule and is designated as an intrinsic relaxation process (IRP). No relaxation phenomenon is observed for temperatures lower than 60 °C (e.g., 20−40 °C). Electrolytes with low salt concentration, i.e., 0.005 M $LiClO_4$−SN, also show behavior similar to pristine

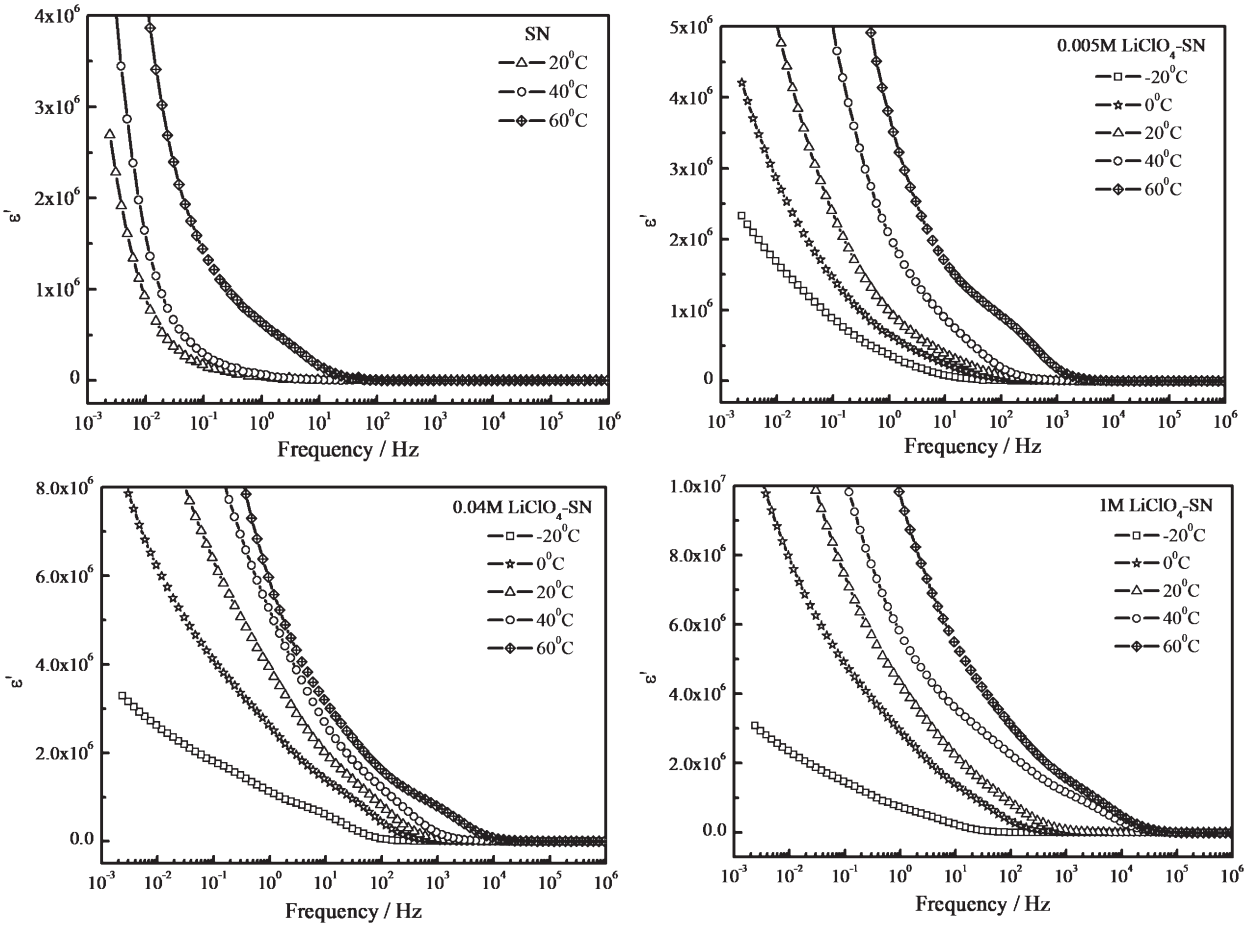

Figure 2. Frequency dependence of the real part of the dielectric permittivity (ε') for 0−1 M $LiClO_4$−SN plastic crystalline electrolytes at different temperatures.

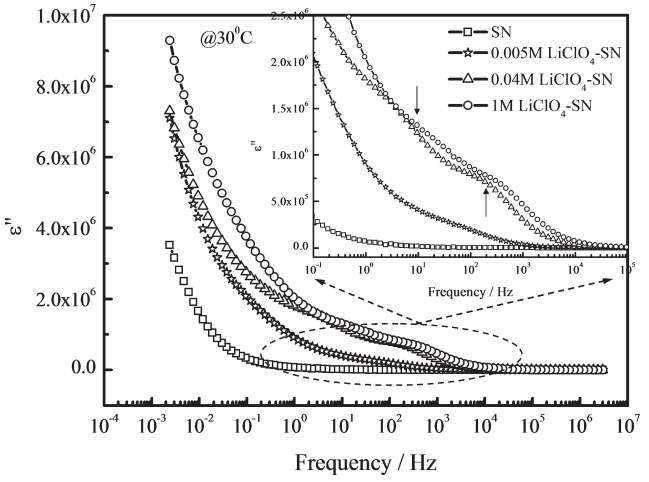

Figure 3. Variation of the imaginary part of the dielectric permittivity value (ε'') as a function of frequency for 0−1 M $LiClO_4$−SN at 30 °C. Intrinsic and salt-induced relaxation processes are indicated by arrow (↓) in the inset of the plot.

SN. In the higher salt concentration regime (x = 0.04−1 M), additional peaks appear, suggesting the presence of additional processes. We address this relaxation process as a salt-induced solvent relaxation process (SISRP). These relaxation processes become more vivid by plotting the imaginary part of the dielectric permittivity, ε'' (dielectric loss), versus frequency, as shown in Figures 3 and 4. Figure 3 shows ε'' versus frequency as a function of salt concentration at 30 °C. ε'' is observed to decrease with increasing frequency from $\sim 2 \times 10^{-3}$ to 10^3 Hz. Higher values of dielectric loss (ε'') at low frequency are due to the contribution of the free charge motion within the electrolyte. A careful inspection of Figure 4 unveils that pristine SN shows only one relaxation peak in the frequency region of ∼1−10 Hz, which becomes pronounced only at higher temperature (60 °C). This is attributed to trans−gauche isomerism of SN molecules. With increasing temperature, lowering of the energy barrier between gauche and trans takes place and this results in a greater number of SN molecules transforming from the gauche to trans phase. The trans phase induces a higher degree of disorder in the sample, leading to faster dynamics. This accounts for the shift in frequency to values with temperature, as shown in Figure 4. The 0.005 M $LiClO_4$−SN sample also displays a single relaxation process in the whole frequency range which becomes more prominent at higher temperature (40−60 °C) due to an increase of the disordered trans phase at high temperature. Similar shifts in frequency are also observed in the case of the 0.005 M $LiClO_4$−SN sample. However, in addition to temperature, the presence of salt (even in dilute amounts) results in the appearance of the peak at lower temperature (≈40 °C) compared to SN and changes in peak contour and position are more vivid. Figures 3 and 4 show two prominent relaxation processes for higher salt concentration (x = 0.04−1 M). The presence of salts

dx.doi.org/10.1021/jp108848b |J. Phys. Chem. B 2011, 115, 2148–2154

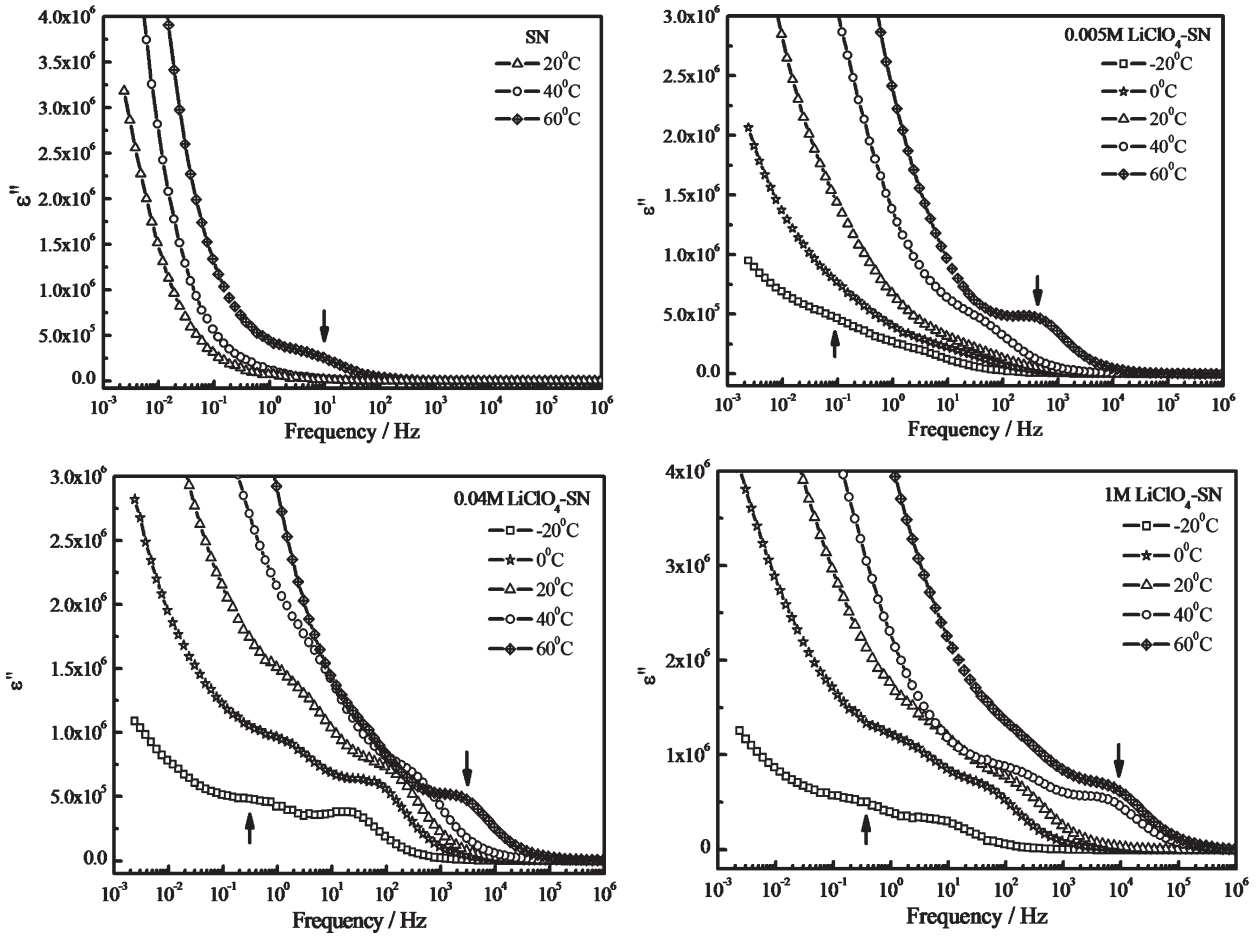

Figure 4. Frequency dependence of imaginary part of dielectric permittivity (ε'') for 0−1 M $LiClO_4$−SN plastic electrolytes at selected temperatures. Relaxation processes are indicated by the sign ↑.

in considerable amounts (∼1 M) reduces further the trans−gauche energy barrier compared to that in pristine SN. This results in higher disorder and an even larger number of SN molecules in the trans state compared to pristine SN and SN with dilute salt concentration. Evidence of these processes at 30 °C suggests strong salt-induced effects on the solvent dynamics. The fast dynamics due to salt and temperature is easily evidenced via a shift in the relaxation peak to higher frequency (∼10^3−10^5 Hz) compared to pristine SN. High fractions of SN molecules reside in the trans phase, resulting in a shift of the IRP to a higher frequency regime (∼5−10^2 Hz at −20 °C to ∼10^3−10^5 Hz at 60 °C) compared to pristine SN (1−10 Hz at 60 °C). The relaxation process (SISRP) is attributed to solvent molecules associated with lithium ion (SN−Li^+) which typically takes place in concentrated electrolytes (0.04−1 M $LiClO_4$−SN). Compared to the intrinsic relaxation process, SISRP appears at much lower frequency, viz., ∼10^{-1}−1 Hz at −20 °C to ∼10−10^3 Hz at 60 °C. This is a slow relaxation process and is also evident from FTIR via the appearance of a band at 627 and 637 cm^{-1}.[21] It is interesting to note from Figure 4 that SISRP becomes more evident with increasing salt concentration and decreasing temperature (due to the presence of a higher fraction of SN−Li^+), whereas an intrinsic relaxation peak is more eminent with an increase of temperature (due to presence of a higher fraction of SN molecules in the trans phase). Both of the relaxation peaks are more pronounced in 0.04 M $LiClO_4$−SN rather than 1 M $LiClO_4$−SN, which may be result from formation of a higher concentration of Li^+−ClO_4^- ion pairs at a high salt concentration. Furthermore the shifting of relaxation peaks toward higher frequencies indicates thermal activation of charge carriers with the increment of temperature.

To better understand the various relaxation processes, the experimental loss spectra were fitted with an empirical model function introduced by Havriliak−Negami (HN function).[28]

$$\varepsilon^*_{HN}(\omega) = \varepsilon_\infty + \frac{\Delta\varepsilon}{(1 + (i\omega\tau_{HN})^\beta)^\gamma}$$

where the symbol ε^* indicates the complex dielectric permittivity, ω (=$2\pi f$) is the angular frequency, τ_{HN} represents the relaxation time, β and γ are shape parameters which describe respectively the symmetric and the asymmetric broadening of the complex dielectric function with the condition $0 < \beta, \beta\gamma \leq 1$, and $\Delta\varepsilon$ is the dielectric relaxation strength with $\Delta\varepsilon = \varepsilon_0 - \varepsilon_\infty$ (ε_0 and ε_∞ are dielectric constant values at $\omega = 0$ and $\omega = \infty$, respectively). For an ideal Debye relaxation process β and γ would be ideally equal to 1. Because space charge polarization is dominant at low frequencies, it was necessary to include the additional contribution of ionic conductivity by adding a term $(-i\sigma)/(\varepsilon_{ev}\omega^s)$ to the dielectric loss, where σ is the direct current (dc) conductivity and ε_{ev} is the dielectric constant of the vacuum; the exponent s ($0 < s \leq 1$) characterizes the conduction process, the conduction is

dx.doi.org/10.1021/jp108848b |J. Phys. Chem. B 2011, 115, 2148–2154

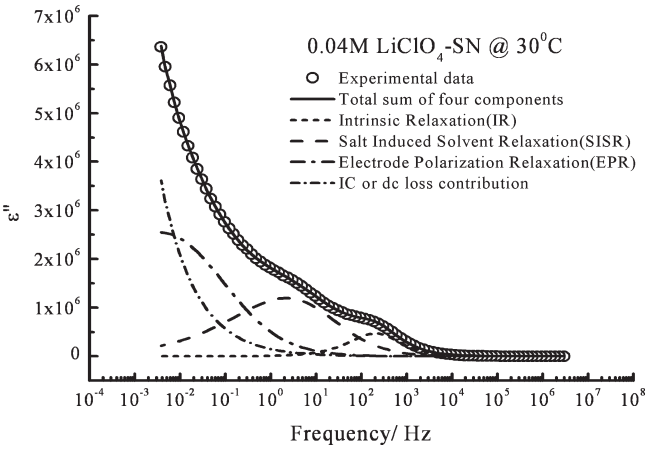

Figure 5. Example of three HN functions and one ionic conductivity (IC) contribution fit of 0.04 M $LiClO_4$−SN at 30 °C. The open circles are experimental data; the solid line is the sum of four fitting components; the dashed and dotted lines are HN function fitting results for three relaxations and dc conductivity.

dominated by ion drift if s = 1, and s = 0.5 suggests strong diffusion-controlled pathways. Multiple HN functions and an ionic conductivity (IC) or dc loss contribution were used to fit the experimental loss curves exhibiting various relaxation processes. Experimental data at 60 °C temperature of pristine SN was fitted using two HN and an IC contribution. Similarly, all temperature data of 0.005 M $LiClO_4$−SN were fitted with two HN functions and an IC. The dielectric data were fitted using multiple Havriliak−Negami functions (cf. Figure 5 and also Supporting Information, Figure S1). For this purpose we have used a standard fitting procedure (χ^2 error minimization using the Levenberg−Marquardt method[29] (Supporting Information, Figure S1). The number of HN functions used for the fitting depended on the concentration and temperature. The spectra of higher concentrations of salt (0.04−1 M $LiClO_4$−SN) were asymmetrically broadened, and in all four functions (three HN and an IC) were observed to fit the data. The additional relaxation process which occurs in the lowest frequency range may be attributed to electrode polarization (EP). In the case of electrolytes with higher salt concentration, accumulation of mobile ions occurs at the electrode interface, leading to large series capacitance and hence a higher dielectric constant. The very large increase of dielectric constant along with extremely high dielectric losses supports this argument for higher salt concentration of plastic crystal electrolytes. Figure 5 displays representative experimental data fitted with three HN functions

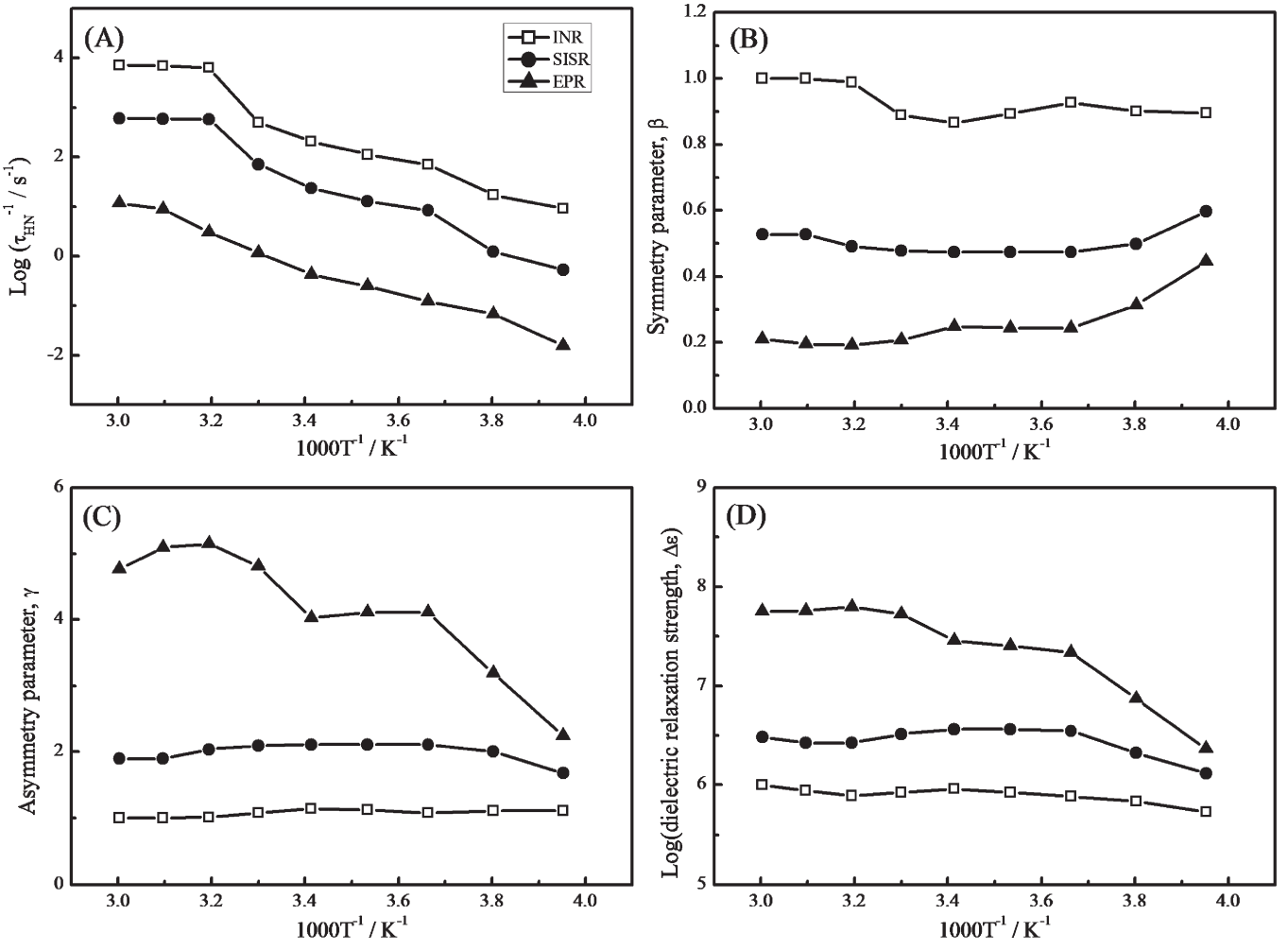

Figure 6. Temperature dependence of three HN fitting parameters for 1 M $LiClO_4$−SN: (A) reciprocal relaxation times ($1/\tau_{HN}$); (B) shape parameters β; (C) shape parameters γ; (D) dielectric relaxation strengths ($\Delta\varepsilon$) for three relaxation processes.

dx.doi.org/10.1021/jp108848b |J. Phys. Chem. B 2011, 115, 2148–2154

and an ionic conductivity contribution (error ~ 1.2%) in case of 0.04 M $LiClO_4$−SN at 30 °C. The best fit HN parameters using the fitting procedure of dielectric loss as a function of temperature are shown in Figure 6 for 1 M $LiClO_4$−SN. Figure 6 (also cf. Supporting Information, Figures S2 and S3) displays the variation of different HN parameters of three different relaxation processes (IRP, SISRP, and EPR) of 1 M $LiClO_4$−SN obtained following the fitting procedure with three HN functions. Figure 6A represents the reciprocal relaxation time ($1/\tau_{HN}$) for three different relaxations (obtained after fitting with three HN functions) as a function of reciprocal temperature of 1 M $LiClO_4$−SN. The relaxation frequency increases with the increase in temperature. As shown in Figure 6D, the dielectric strength ($\Delta\varepsilon$) is higher for electrode polarization relaxation process (EPRP) than SISRP and IRP. The dielectric strength, $\Delta\varepsilon$, increases strongly with temperature for EPRP, whereas it remains constant in the case of SISRP and IRP processes in the entire temperature range (Figure 6D) which is attributed to an increase in the number of mobile ionic species. The HN parameter β is a function of both composition and temperature. In Figure 6B the smaller value of β (higher value of γ (Figure 6C)) indicates a broader and asymmetric peak for EPR processes. It shows a non-Debye type nature for the present electrolyte system. A similar trend was also observed for 0.04 M $LiClO_4$−SN (cf. Supporting Information, Figure S3). The non-Debye type response is also clearly evident from dielectric tangent loss (tan δ) versus a frequency plot at different salt concentration (constant temperature = 30 °C). The maximum in tan δ shifts to higher frequency (lower relaxation time) with an increase in salt concentration (cf. Supporting Information, Figure S4), and peaks are asymmetrical for x M $LiClO_4$−SN (x = 0.005−1). This is attributed to the increase in concentration of the disordered trans phase in plastic crystalline electrolytes as discussed earlier. The nonsymmetrical curves indicate a non-Debye relaxation[30,31] and the presence of multiple relaxation processes. This nonsymmetric shape can also be accounted for by a stretched exponential decay relaxation function defined empirically by the Kohlrausch−Williams−Watta (KWW) function[32] in the time domain as

$$\phi(t) = \exp\left[-\left(\frac{t}{\tau_{KWW}}\right)^{\beta_{KWW}}\right]$$

where τ_{KWW} is the relaxation time and β_{KWW} is the Kohlrausch exponent also known as the stretching parameter; β_{KWW} can be calculated from the following equation β_{KWW} = 1.14/FW (FW, full width at half-maximum). For simple Debye relaxation behavior, the response is an exponential function with β_{KWW} = 1, whereas β_{KWW} < 1 implies deviation from the Debye relaxation process. Additional attempts at analysis of the dielectric data using KWW was not possible due to several reasons. Usually KWW analysis (i.e., estimation of τ_{KWW} and β_{KWW}) is done using fits to the electric modulus data (M' and M'').[33,34] In our case the peak in M'' appears only at low temperatures around −20 °C. At −20 °C β_{KWW} was estimated to be ≈0.77 for 1 M $LiClO_4$−SN, suggesting a non-Debye type relaxation process in $LiClO_4$−SN electrolytes (cf. Supporting Information, Figure S6). At higher temperatures the peak is expected to shift to even higher frequencies, higher than 1 MHz (implying even lower τ_{KWW}; cf. Supporting Information, Figure S7). This is presently beyond our infrastructural capabilities. The decrease in relaxation time (extracted from the tan δ versus frequency plot) with temperature again reveals an increase in the disordered trans phase and increment in the number of charge carriers. Relaxation time ($\tau = 1/2\pi f_{max}$) fitted to Arrhenius equation ($\tau = \tau_0 e^{E_a/KT}$) is shown in Figure 7. The activation energy (E_a) increases from 0.23 eV for pristine SN to 0.54 eV for 1 M $LiClO_4$−SN. These E_a values calculated from dielectric tangent loss factor are very much similar to those reported from ionic conductivity measurements.[21] An increase in E_a is attributed to considerable ion association taking place at higher salt contents.

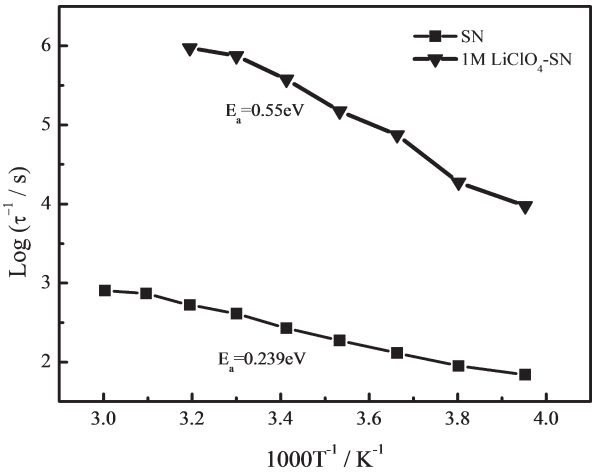

Figure 7. Reciprocal relaxation time as a function of reciprocal temperature for pristine plastic crystal (SN) and plastic crystal electrolyte (1 M $LiClO_4$−SN).

4. CONCLUSIONS

The various relaxation processes influencing the ion transport mechanism in succinonitrile−lithium salt electrolytes were convincingly demonstrated via detailed dielectric relaxation studies. All relaxation processes were found to be dependent on temperature and salt concentration. The increment in the number of relaxation processes in moving from pristine SN to $LiClO_4$−SN electrolytes suggests the important role of ion solvation and solvent−salt interaction on ion transport. The relaxation processes visible from the dielectric measurement could be well-accounted for by the Havriliak−Negami function, while the tan δ analyzed using KWW resulted in E_a estimates at far with detailed ionic conductivity studies reported earlier. The present study again confirms and supplements our line of approach of employing solution chemistry based concepts over conventional solid-state (defect) chemistry in comprehension of ion transport in organic plastic crystalline solids. Fundamental studies such as this will further facilitate design of electrolytes for electrochemical applications such as rechargeable lithium-ion batteries.

■ ASSOCIATED CONTENT

Supporting Information. Procedure for fitting of dielectric data with two/three HN functions and one IC contribution using a standard fitting procedure (χ^2 error minimization using Levenberg−Marquardt Method (Figure S1), temperature dependence of two HN fitting parameters for 0.005 M/0.04 M $LiClO_4$−SN, viz., reciprocal relaxation times ($1/\tau_{HN}$), shape parameters β, shape parameters γ, and dielectric relaxation strengths ($\Delta\varepsilon$) for three different relaxation processes (Figures S2 and S3), variation of dielectric tangent loss (tan δ) with

frequency for 0−1 M $LiClO_4$−SN and normalized plot of (tan δ/tan δ_{max}) versus (f/f_{max}) for all samples (Figure S4), tan δ versus frequency at different temperatures for 0.04 M $LiClO_4$−SN and 1 M $LiClO_4$−SN (Figure S5), real (M') and imaginary (M'') parts (including fitting) of the electric modulus as a function of frequency at temperature −20 °C (Figure S6), imaginary (M'') parts of the electric modulus as a function of frequency at various temperatures (Figure S7). This material is available free of charge via the Internet at http://pubs.acs.org.

AUTHOR INFORMATION

Corresponding Author

*E-mail: aninda_jb@sscu.iisc.ernet.in. Tel.: +91 80 22932616. Fax: +91 80 23601310.

ACKNOWLEDGMENT

A.J.B. acknowledges DST, Government of India, for research funding. S.D. thanks CSIR for Senior Research Fellowships.

REFERENCES

(1) Fenton, D. E.; Parker, J. M.; Wright, P. V. *Polymer* **1973**, *14*, 589.
(2) Abouimrane, A.; Davidson, I. J. *J. Electrochem. Soc.* **2007**, *154*, A1031.
(3) Berthier, C.; Gorecki, W.; Minier, M.; Armand, M. B.; Chabagno, J. M.; Rigaud, P. *Solid State Ionics* **1983**, *11*, 91.
(4) Ratner, M. A.; Shriver, D. F. *Chem. Rev.* **1988**, *88*, 109.
(5) Macfarlane, D. R.; Forsyth, M.; Howlett, P. C.; Pringle, J. M.; Sun, J.; Annat, G.; Neil, W.; Izgorodina, E. I. *Acc. Chem. Res.* **2007**, *40*, 1165.
(6) Galinski, M.; Lewandowski, A.; Stepniak, I. *Electrochim. Acta* **2006**, *51*, 5567.
(7) Croce, F.; Appetecchi, G. B.; Persi, L.; Scrosati, B. *Nature* **1998**, *394*, 456.
(8) Armand, M.; Tarascon, J. M. *Nature* **2008**, *451*, 652.
(9) Guo, Y. G.; Hu, J. S.; Wan, L. J. *Adv. Mater.* **2008**, *20*, 4384.
(10) Xu, K. *Chem. Rev.* **2004**, *104*, 4303.
(11) Appetecchi, G. B.; Aihara, Y.; Scrosati, B. *Solid State Ionics* **2004**, *170*, 63.
(12) MacFarlane, D. R.; Forsyth, M. *Adv. Mater.* **2001**, *13*, 957.
(13) Long, S.; MacFarlane, D. R.; Forsyth, M. *Solid State Ionics* **2003**, *161*, 105.
(14) Alarco, P. J.; Abu-Lebdeh, Y.; Abouimrane, A.; Armand, M. *Nat. Mater.* **2004**, *3*, 476.
(15) Patel, M.; Menezes, P. V.; Bhattacharyya, A. J. *J. Phys. Chem. B* **2010**, *114*, 5233.
(16) Long, S.; MacFarlane, D. R.; Forsyth, M. *Solid State Ionics* **2004**, *175*, 733.
(17) Aronsson, R.; Jansson, B.; Knape, H. E. G.; Lunden, A.; Nilsson, L.; Sjoblom, C. A.; Torell, L. M. *J. Phys., Colloq.* **1979**, *C6*, 35.
(18) Tansho, M.; Furukawa, Y.; Nakamura, D.; Ikeda, R. *Ber. Bunsen-Ges.* **1992**, *96*, 550.
(19) Lukac, P. *Plasticity of Metals and Alloys*; Proceedings of the 6th International Symposium on Plasticity of Metals and Alloys (ISPMA-6), Prague, Czech Republic, September 1994; Trans Tech: Zurich, Switzerland, 1994.
(20) Sherwood, J. N. *The Plastically Crystalline State: Orientationally Disordered Crystals*; Wiley: London, 1979.
(21) Das, S.; Prathapa, S. J.; Menezes, P. V.; Row, T. N. G.; Bhattacharyya, A. J. *J. Phys. Chem. B* **2009**, *113*, 5025.
(22) Derollez, P.; Lefebvre, J.; Descamps, M.; Press, W.; Fontaine, H. *J. Phys.: Condens. Matter* **1990**, *2*, 6893.
(23) Alvarez, C.; Sics, I.; Nogales, A.; Denchev, Z.; Funari, S. S.; Ezquerra, T. A. *Polymer* **2004**, *45*, 3953.
(24) Jin, X.; Zhang, S. H.; Runt, J. *Macromolecules* **2004**, *37*, 4808.
(25) Natesan, B.; Karan, N. K.; Rivera, M. B.; Aliev, F. M.; Katiyar, R. S. *J. Non-Cryst. Solids* **2006**, *352*, 5205.
(26) Ramya, C. S.; Selvasekarapandian, S.; Hirankumar, G.; Savitha, T.; Angelo, P. C. *J. Non-Cryst. Solids* **2008**, *354*, 1494.
(27) Agrawal, S. L.; Awadhia, A. *Bull. Mater. Sci.* **2004**, *27*, 523.
(28) Kremer, F.; Schonhals, A. *Broadband Dielectric Spectroscopy*; Springer-Verlag: Berlin, Germany, 2002.
(29) Press, W. H.; Teukolsky, S. A.; Vetterling, W. T.; Flannery, B. P. *Flannery Numerical Recipes in Fortran 77: The Art of Scientific Computing*, 2nd ed.; Cambridge University Press: Cambridge, U.K., 1992; Chapter 15, p 678.
(30) Hill, R. M.; Dissado, L. A. *J. Phys. C: Solid State Phys.* **1985**, *18*, 3829.
(31) Jonscher, A. K. *J. Phys. D: Appl. Phys.* **1999**, *32*, R57.
(32) Willams, G.; Watts, D. C.; Dev, S. B.; North, A. M. *Trans. Faraday Soc.* **1971**, *67*, 1323.
(33) Vaish, R.; Varma, K. B. R. *J. Electrochem. Soc.* **2009**, *156*, G17.
(34) Vaish, R.; Varma, K. B. R. *J. Appl. Phys.* **2009**, *106*, 064106.